Atmos. Chem. Phys., 11, 9037–9052, 2011
www.atmos-chem-phys.net/11/9037/2011/
doi:10.5194/acp-11-9037-2011

Atmospheric Chemistry and Physics

Black carbon aerosol mixing state, organic aerosols and aerosol optical properties over the United Kingdom

G. R. McMeeking[1,*], W. T. Morgan[1], M. Flynn[1], E. J. Highwood[2], K. Turnbull[3], J. Haywood[3,4], and H. Coe[1]

[1]Centre for Atmospheric Science, University of Manchester, Manchester, UK
[2]Department of Meteorology, University of Reading, Reading, UK
[3]The Met Office, Exeter, UK
[4]CEMPS, University of Exeter, Exeter, UK
[*]now at: Dept. of Atmospheric Science, Colorado State University, Fort Collins, CO, USA

Received: 27 April 2011 – Published in Atmos. Chem. Phys. Discuss.: ACPD 17 May 2011
Revised: 8 August 2011 – Accepted: 29 August 2011 – Published: 5 September 2011

Abstract. Black carbon (BC) aerosols absorb sunlight thereby leading to a positive radiative forcing and a warming of climate and can also impact human health through their impact on the respiratory system. The state of mixing of BC with other aerosol species, particularly the degree of internal/external mixing, has been highlighted as a major uncertainty in assessing its radiative forcing and hence its climate impact, but few in situ observations of mixing state exist. We present airborne single particle soot photometer (SP2) measurements of refractory BC (rBC) mass concentrations and mixing state coupled with aerosol composition and optical properties measured in urban plumes and regional pollution over the United Kingdom. All data were obtained using instrumentation flown on the UK's BAe-146-301 large Atmospheric Research Aircraft (ARA) operated by the Facility for Airborne Atmospheric Measurements (FAAM). We measured sub-micron aerosol composition using an aerosol mass spectrometer (AMS) and used positive matrix factorization to separate hydrocarbon-like (HOA) and oxygenated organic aerosols (OOA). We found a higher number fraction of thickly coated rBC particles in air masses with large OOA relative to HOA, higher ozone-to-nitrogen oxides (NO_x) ratios and large concentrations of total sub-micron aerosol mass relative to rBC mass concentrations. The more ozone- and OOA-rich air masses were associated with transport from continental Europe, while plumes from UK cities had higher HOA and NO_x and fewer thickly coated rBC particles. We did not observe any significant change in the rBC mass absorption efficiency calculated from rBC mass and light absorption coefficients measured by a particle soot absorption photometer despite observing significant changes in aerosol composition and rBC mixing state. The contributions of light scattering and absorption to total extinction (quantified by the single scattering albedo; SSA) did change for different air masses, with lower SSA observed in urban plumes compared to regional aerosol (0.85 versus 0.9–0.95). We attribute these differences to the presence of relatively rapidly formed secondary aerosol, primarily OOA and ammonium nitrate, which must be taken into account in radiative forcing calculations.

Correspondence to: G. McMeeking
(gavin@atmos.colostate.edu)

1 Introduction

The optical properties of atmospheric aerosols play a major role in determining their impacts on climate (Haywood and Osborne, 2000). Aerosol optical properties depend on the physical (e.g., size and shape) and chemical (e.g., composition, mixing state) character of the particles and both transform in the atmosphere. The changes also alter the hygroscopicity of the particles, which determines how readily they serve as cloud condensation nuclei (CCN) or ice nuclei (IN), and are related to the aerosol atmospheric lifetime. For example, black carbon (BC) particles that acquire coatings may absorb light more efficiently (e.g., Fuller et al., 1999; Bond and Bergstrom, 2006; Lack et al., 2009; Moffet and Prather, 2009; Lack and Cappa, 2010; Shiraiwa et al., 2010) and be more prone to wet scavenging processes and have a shorter atmospheric lifetime (e.g., Wyslouzil et al., 1994; Weingartner et al., 1997; Zhang et al., 2008; Riemer et al., 2010; Zaveri et al., 2010; McMeeking et al., 2011a) compared to their non-coated counterparts.

Published by Copernicus Publications on behalf of the European Geosciences Union.

Recently Morgan et al. (2010a) showed that organic aerosols (OA), which globally make up 20–90 % of submicron aerosol mass (Zhang et al., 2007), could be represented as a continuum of oxygenated OA (OOA), with significant chemical processing downwind of major source regions over Europe. Jimenez et al. (2009) showed that such behavior could be described by a unified modeling framework, the 2-D volatility basis set, and stated that future work would need to account for the dynamic sources and sinks of OA to make accurate regional and global predictions of OA. Other advances in modeling treatments of aerosol micro-physical properties, including size and mixing state, have improved the physical basis for predicting aerosol optical properties and lifetime on regional and global scales (Koch et al., 2009; Jacobson, 2010; Zaveri et al., 2010). The improvements are particularly important for predicting aerosol light absorption, which depends on the mixing state and size of BC as well as its abundance.

Advances in instrumentation have provided single particle data that give a direct measure of mixing state and provide a test and constraint for model micro-physical schemes. Single particle aerosol mass spectrometry approaches provide detailed chemical composition measurements including BC (Moffet and Prather, 2009; Pratt and Prather, 2010; Dall'Osto et al., 2010) and single particle soot photometers (SP2) provide mixing state information specific to refractory BC (rBC) in addition to mass quantification (Schwarz et al., 2006; Shiraiwa et al., 2007; Schwarz et al., 2008a; Subramanian et al., 2010). In Europe, Baumgardner et al. (2008) measured rBC in the upper troposphere-lower stratosphere (UT-LS) region and McMeeking et al. (2010) measured rBC in the boundary layer with airborne SP2 instruments, but neither examined the rBC mixing state. Surface-based SP2 measurements in Europe are also relatively limited to date. Liu et al. (2010) used an SP2 to measure rBC mixing at a high alpine site in Switzerland and Liu et al. (2011) performed similar measurements downwind of Manchester in the United Kingdom. Dall'Osto et al. (2010) measured single particle composition at Mace Head, Ireland using an aerosol time-of-flight mass spectrometer (ATOFMS) and found that aerosols in air masses originating from northern Europe were enriched in potassium, elemental carbon (similar to BC) and nitrate while those passing over France and Spain were enriched in organic carbon and sulfate.

Our work is closely related to three previous studies in which we examined the evolution of OA over Europe (Morgan et al., 2010a), the distribution and size of rBC over Europe (McMeeking et al., 2010) and the relationship between aerosol optical properties and semi-volatile aerosol components (Morgan et al., 2010b). Here we link recent advances in the treatment of OA and rBC mixing state to examine relationships between the evolution of OA, rBC mixing state, and their subsequent impacts on aerosol optical properties using airborne measurements of rBC, aerosol composition and aerosol optical properties. The results are the first measurements of rBC mixing state aloft over Europe. We also compare our findings to previous aircraft-based observations in other locations.

2 Method

All measurements reported here were made from the UK's BAe-146-301 large Atmospheric Research Aircraft operated by the Facility for Atmospheric Airborne Measurements (FAAM). We performed 14 research flights to examine the transformation of trace gases and particles emitted from major source regions in the UK as part of the APPRAISE-ADIENT (Aerosol properties, processes and influences on the Earth's climate system – Appraising the aerosol direct impact on climate) and EM25 (Emissions around the M25 motorway) projects. Our analysis focuses on measurements performed on 16 April 2008 and 24 June 2009 that aimed to characterize emissions from urban centers in the absence of significant cloud processing of the aerosol. These dates were the only periods when meteorological conditions in regions where the aircraft was allowed to operate were suited to our objectives. McMeeking et al. (2010) presents a broader overview of rBC observations during the other flights in the campaigns. We describe the major instrument systems operating on the aircraft relevant to this work below.

2.1 Single particle soot photometer

McMeeking et al. (2010) described the SP2, inlets, calibration and data analysis procedures used in this study in detail, so here we only discuss aspects of the analysis relevant to rBC mixing state and coating properties. We treat rBC-containing particles as rBC "cores" coated by "shells" of other material. The SP2 (DMT Inc., Boulder, CO, USA) provided information about both the mass of the rBC "core" (if present) and the amount of additional coating for each particle detected. It relied on a laser-induced incandescence technique (Stephens et al., 2003) to identify and quantify rBC mass in individual particles over a nominal rBC mass range of approximately 0.5–300 fg (mass equivalent diameter range 80–680 nm for assumed rBC density of 1.8 g cm^{-3}) depending on the instrument configuration. Two avalanche photodetectors measured light scattered by particles passing through the laser, which were related to particle size through PSL calibrations. Particles containing sufficient absorbing material evaporated in the beam (causing the scattering signal to degrade) and eventually the rBC core vaporized and emitted light that was related to the rBC core mass. The rBC mass response was determined using mobility-selected Aquadag (16 April 2008) and glassy carbon spheres (24 June 2009).

The initial information obtained for each particle (after the calibration had been applied) can be summarized as: (a) whether or not the particle contains a detectable mass of rBC and, if so, the quantity of that mass, (b) the light

scattering-derived size of both rBC and non-rBC containing particles with optical diameters between approximately 200–450 nm, and (c) the time elapsed between the peak of the incandescence and scattering signals. Refractory BC mass information was available over a wider size range than scattering information due to the limited sensitivity and saturation of the detectors. The size range depended on detector gain settings and the optical properties of individual particles and in our study was approximately 200–450 nm diameter (based on polystyrene latex sphere calibration). We determined the number fraction of "thickly coated" rBC particles (f) based on the time delay between incandescence and scattering signal peaks for the entire ensemble of rBC containing particles with scattering responses within the detection range and for specific rBC core diameter ranges (Schwarz et al., 2006; Shiraiwa et al., 2007). The time criterion was based on the observed minimum in the bimodal frequency distribution of delay times (Moteki et al., 2007). Moteki and Kondo (2007) found an abrupt increase in the time delay at a threshold total particle diameter-to-BC core diameter ratio of 2 ± 0.5. We did not observe significant differences in f for different rBC core diameter ranges, so unless otherwise stated reported f is for the entire rBC distribution with detectable light scattering signals.

2.2 Aerosol mass spectrometer

A compact Time-of-Flight aerosol mass spectrometer (AMS; Aerodyne Inc., Billerica, MA, USA) measured sub-micron aerosol chemical composition at approximately 30 s time resolution (Drewnick et al., 2005) for level flight and approximately 10 s resolution for ascents and descents in most cases. The AMS provided sub-micron, non-refractory aerosol composition and mass information, including OA, sulfate, nitrate, and ammonium concentrations. Morgan et al. (2010a) described the inlets, instrument calibration and data anlaysis procedures, including the positive matrix factorization (PMF) technique used to interpret the organic mass spectra (Ulbrich et al., 2009). Aerosol mass concentrations were compared to light scattering coefficients and other aerosol mass concentration proxies to verify data quality and correct application of the composition-dependent AMS collection efficiency (Morgan et al., 2010a; Matthew et al., 2008).

Positive matrix factorization (Paatero and Tapper, 1994; Paatero, 1997) analysis of the AMS data was performed here in order to further interpret the sources and processing of OA. Several previous publications (e.g., Ulbrich et al., 2009; Allan et al., 2010; Morgan et al., 2010a) give details for the application of PMF to AMS organic mass spectra. PMF was used in this analysis in order to separate hydrocarbon-like OA (HOA) and oxygenated OA (OOA) contributions to the OA burden and we wished to examine their relative importance in pollution plumes. Furthermore, previous studies have often separated the OOA fraction into sub-sets related to their age and volatility, which may be of importance here when comparing regional scale pollution to more locally derived pollution plumes.

The PMF solution for the 16 April 2008 case study has been previously reported in Morgan et al. (2010a). Briefly, a two factor solution was chosen comprised of HOA and low volatility-OOA (LV-OOA) (Jimenez et al., 2009) based on their correlation with external tracers, resemblance to reference mass spectra and the mathematical robustness of the solution. The PMF solution for 24 June 2009 is reported here for the first time, but similar criteria were used to select the solution as for the 16 April 2008 case, with both using procedures outlined in Ulbrich et al. (2009). The solution had three factors; HOA, semi-volatile-OOA (SV-OOA) and LV-OOA. A two factor solution was not deemed appropriate as this resulted in an ambiguous separation between HOA and OOA. Solutions with greater than three factors led to factors being split into several numerically similar factors. Consequently, the three factor solution provided a separation between the HOA and OOA components, while also providing a more robust distinction between the SV-OOA and LV-OOA components.

The rotational freedom of the three factor solution was explored via variation of a parameter known as fPeak. An fPeak value of zero was used for the three factor solution based upon the resemblance of the HOA factor to both reference mass spectra and primary combustion tracers. Correlation coefficients of 0.69 and 0.73 between HOA and carbon monoxide (CO) and rBC respectively were determined for an fPeak of zero. Correlation coefficients of 0.68 and 0.63 were observed for fPeak = 0.5. The numerical stability of the three factor solution was tested based upon a bootstrapping analysis (Ulbrich et al., 2009), where random re-sampling of the data matrix is performed in the time dimension. Furthermore, little variation in the factor solutions was observed when a range of initiation seeds was used.

2.3 Other instruments and tools

Aerosol light scattering and absorption coefficients were measured by an integrating nephelometer (TSI 3563, St. Paul, MN, USA) and particle soot absorption photometer (PSAP, Radiance Research, Boulder, CO, USA). Measured aerosol light scattering coefficients were corrected for artifacts from truncation and the non-lambertian light source in the nephelometer using the sub-micron aerosol parameters provided by Anderson and Ogren (1998). Light scattering coefficients were measured at λ = 450, 550 and 700 nm, but we only discuss the 550 nm measurements. Measured aerosol light absorption coefficients were corrected for artifacts associated with filter spot size, flow rate and the presence of scattering particles on the filter following Bond et al. (1999) and Ogren (2010). We removed PSAP data from the analysis when the aircraft was changing altitude or flying through clouds. The aircraft does not have an active drying system, however heating of the sample when it was drawn

into the cabin acted to dry the sample. Our best estimate of the sample relative humidity (RH) for the optical instruments was measured at the nephelometer and was <35 % for the April 2008 flight, but higher for the first (∼60 %) and second (∼40 %) June 2009 flights.

All aerosol measurements including optical coefficients are reported at standard temperature and pressure (STP; temperature = 273.15 K and pressure = 1013.25 hPa) and denoted by an "s" for clarity (e.g., $\mu g\,sm^{-1}$). Gas-phase concentrations of CO (Aero-Laser AL5002), ozone (O_3; Thermo Model 49C), and nitrogen oxides (NO_x; Thermo Model 42) were measured by VUV resonance fluorescence, UV photometry, and chemiluminescence, respectively. Our reported NO_x was a surrogate for nitrogen oxides mixing ratios in that it was operationally defined as any species converted to NO under a heated (325 °C) molybdenum catalyst. All data were averaged to the AMS sampling interval. All reported measurements refer to observations in the boundary layer unless otherwise stated.

We examined the large-scale meteorological transport patterns using a combination of visible and infrared satellite imagery, the re-analysis from the European Centre for Medium-Range Weather Forecasting (ECMWF) ERA interim product, backward trajectory modeling, and the Met Office operational numerical weather prediction (NWP) UK4 forecasting model. We ran 72-hour backward trajectories from different locations along the flight path using the NOAA HYSPLIT Lagrangian transport model (Draxler and Rolph, 2011; Rolph, 2011) with modeled vertical velocities.

In addition to providing standard meteorological variables such as temperature, humidity, cloud and precipitation fields, the UK4 model includes a highly simplified representation of aerosol emission, transformation, and deposition (Clark et al., 2008). Sources of aerosol are based on the European emission inventory on a 1/8 degree by 1/16 degree grid developed for the Global and regional Earth-system (Atmosphere) Monitoring using Satellite and in-situ data (GEMS) project by Visschedijk et al. (2007) plus ship emissions from the European Monitoring and Evaluation Programme (EMEP) emissions database for 2005. The aerosol is represented by a single tracer (known as murk) which approximately accounts for emissions sources from SO_2, NO_x and VOCs by using a conversion factor representing the average conversion of the emissions to aerosol within the model domain. The aerosol concentration is used along with a mean hygroscopic growth factor to provide forecasts of atmospheric visibility (Koschmieder, 1924; Haywood et al., 2008). The hygroscopic growth factor used is based on nephelometer data from previous flight campaigns (Haywood et al., 2008). Variational data-assimilation of observed visibilities are used to correct the model fields of aerosol mass concentration and relative humidity (Clark et al., 2008).

3 Results and discussion

3.1 Meteorology and transport

We examined rBC mixing state and other aerosol properties in detail for two case studies, which took place on 16 April 2008 between approximately 10:00–15:00 UTC and 24 June 2009 between approximately 09:00–17:00 UTC. Meteorological conditions were similar on both days (Fig. 1a and b), with high pressure over Scandinavia resulting in easterly/southeasterly anti-cyclonic flow over the UK. The 16 April case study (referred to as the April case study) was a single flight operating mainly in the Irish Sea downwind of northwestern England and the Welsh coast (Fig. 1c). The 24 June case study involved two flights (referred to as the June case study). The first circled the greater London area before performing a westward leg over the English Channel. The second flight took off from southwestern England and flew north towards the Irish Sea where we flew a plume mapping pattern similar to the April flight (Fig. 1d).

The 16 April 2008 flight took place shortly after the passage of a weak cold front and associated precipitation over the north of England on the night of 15 April. The low-level flow became southeasterly following the passage of the front, advecting pollution from northwestern England over the Irish Sea. There were scattered low-level clouds over land covering most of the UK on the 16 April, but the aircraft did not sample in these areas. The 24 June 2009 flight took place when a high pressure system moved eastwards across the UK towards Scandinavia. The system was roughly centered over the UK on 23 June and over the Atlantic Ocean southwest of Ireland on 22 June. The 24 June flights took place during almost completely cloud free conditions over the UK.

Aerosol mass fields predicted by the UK4 visibility model provided an indication of the locations of plumes and their sources during the flights. Figure 1c shows a well-defined plume moving northwest from the Liverpool/Manchester region, extending as far as the Irish coast. The majority of the April flight focused on this plume, but the aircraft also encountered a second, weaker plume in the Bristol Channel, which was also evident in the UK4 forecast (Fig. 1c), and that originated from the Bristol and southern Wales region. The transport pattern on the 24 June flight was similar, but the flow was slightly more easterly than south-easterly over the Irish Sea. There was a large region of elevated concentrations over the southern Irish Sea to the west of Wales. The Manchester/Liverpool plume appeared to mix with a second plume originating further to northeast, near the Kingston Upon Hull (Hull) region. The plume's source appeared to be related to emissions from industrialized regions near Hull with additional contributions from several coal-fired power stations in the area. Pollution around the greater London area was also sampled during the morning flight on 24 June. The flight followed a roughly circular route around London as part of a series of flights examining pollution in and around the Greater

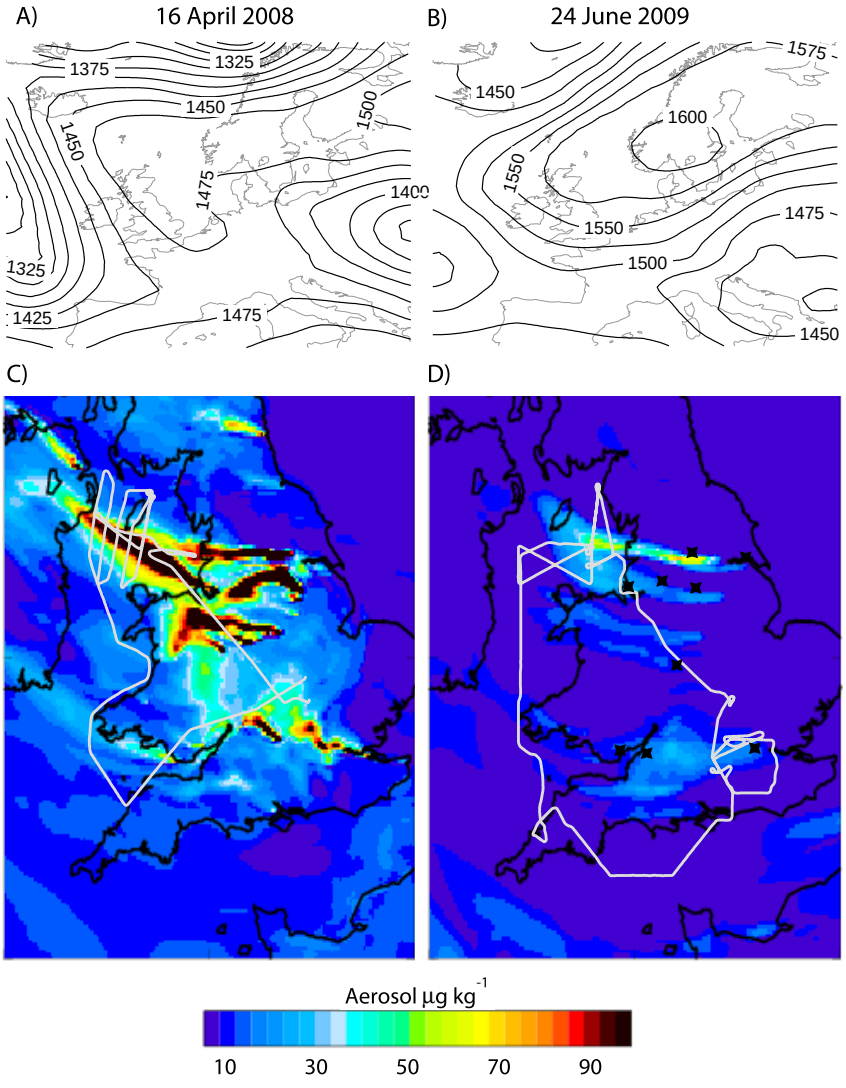

Fig. 1. Geopotential height fields at the 850 hPa pressure level from the ECMWF ERA interim reanalysis at 12:00 UTC for the 16 April 2008 **(a)** and 24 June 2009 **(b)**. Panels **(c** and **d)** show the aircraft flight tracks in white overlaying the UK4 visibility model-predicted aerosol mass fields at the approximate level of the aircraft (approximately 200 m a.s.l. on 16 April and 680 m a.s.l. on 24 June) for periods when the aircraft was flying in the northwestern plumes. The locations of major UK cities are shown by black crosses in panel **(d)**. See Fig. 2 for labels.

London area, which are described in more detail elsewhere (McMeeking et al., 2011b).

3.2 Ozone, carbon monoxide and nitrogen oxides

Operational background CO mixing ratios were determined from the relationships between rBC, NO_x and CO, defined as the average y-intercept of the regression of CO on rBC and NO_x, and were 150 ± 10 ppb for the April flight and 90 ± 10 ppb for the June flight. Novelli et al. (1998) showed that the seasonal cycle of CO at Mace Head, Ireland, a background site at roughly the same latitude as our flight area, decreased from a springtime maximum of approximately 150 ppb to a summertime minimum of 80–90 ppb. Lower summertime CO background mixing ratios generally result from increased hydroxyl radical concentrations in the summer that increase the removal rate of CO. Novelli et al. (1998) also used a box model to simulate the seasonal CO cycle and found that it was driven by changes in hydroxyl concentrations and emissions from biomass burning. Carbon monoxide mixing ratios increased by approximately 150 ppb and 50 ppb in plumes encountered during the April and June case studies, respectively. NO_x mixing ratios increased from background levels of roughly 2 ppb to mixing ratios as high as 30–40 ppb in April and to 10–15 ppb in June in plumes, shown in Table 1. Ozone concentrations ranged

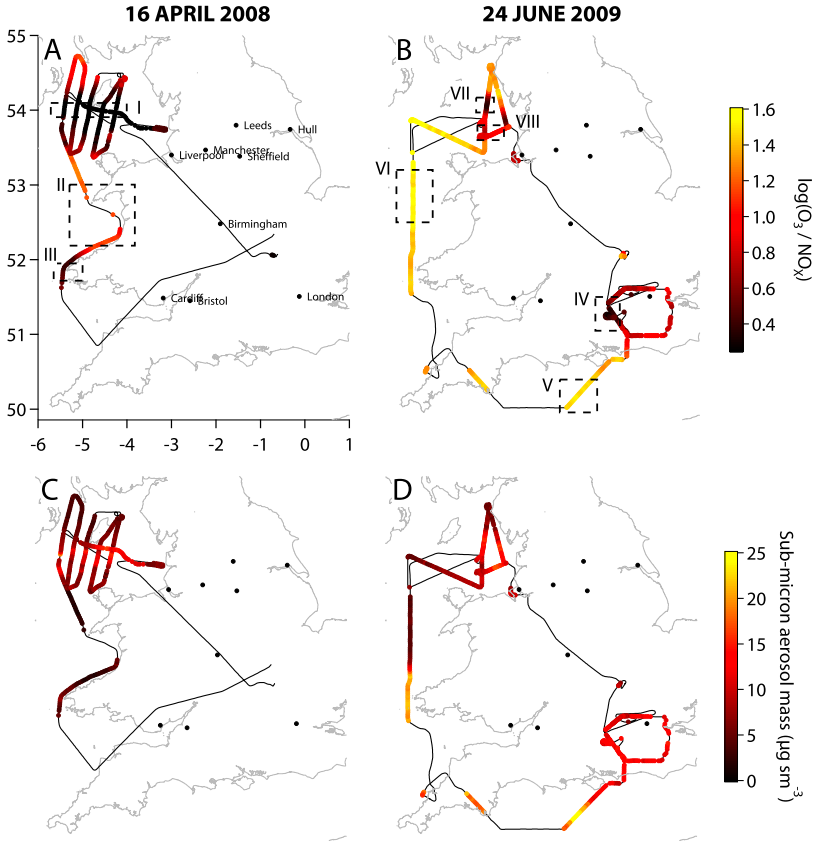

Fig. 2. Maps showing the ratio of ozone-to-nitrogen oxides mixing ratios **(a–b**, note logarithm scale) and sub-micron aerosol mass concentrations measured by the AMS and SP2 **(c–d)**. Only periods when the aircraft was flying at a level altitude in the boundary layer are highlighted. Solid black line shows the flight track. Locations of major cities and selected regions are also indicated.

Table 1. Mixing ratios of ozone and nitrogen oxides, aerosol mass concentrations, and the number fraction of thickly coated refractory black carbon particles (f) averaged over air mass boxes identified in Fig. 2.

Box ID	O_3 (ppb)	NO_x (ppb)	OA ($\mu g\,sm^{-3}$)	sulfate ($\mu g\,sm^{-3}$)	nitrate ($\mu g\,sm^{-3}$)	ammonium ($\mu g\,sm^{-3}$)	rBC ($\mu g\,sm^{-3}$)	total ($\mu g\,sm^{-3}$)	f
I. Liverpool plume	28	29	1.3	2.2	3.7	1.9	0.4	9.5	0.16
II. Background	43	3	0.8	0.9	0.9	0.6	0.1	3.3	0.32
III. Bristol plume	38	13	1.1	1.3	2.0	1.1	0.2	5.7	0.23
IV. London plume	37	13	3.7	3.2	2.9	2.0	0.6	12.0	0.18
V. European outflow	51	4	4.6	4.4	4.6	2.8	0.2	16.3	0.37
VI. Background	46	1	2.1	1.4	0.4	0.6	0.1	4.5	0.27
VII. NW plume 1	39	7	2.6	4.8	2.7	2.5	0.3	12.9	0.27
VIII. NW plume 2	49	5.9	3.4	3.1	2.5	1.8	0.4	11.0	0.21

from 35–50 ppb in April and 30–60 ppb in June, with the larger values observed in regions not influenced by the urban plumes, also shown in Table 1. The lower ozone concentrations in the plumes were consistent with titration of ozone by high NO_x concentrations.

We used the mixing ratios of O_3 and NO_x to assess the photochemical environment during the flights. Figures 2a and 2b show ratios of O_3 to NO_x measured along the flight tracks for level runs below 1 km altitude. For April, the ratio was lowest off the western Welsh coast (Box III in Fig. 2a) and Irish Sea (Box I in Fig. 2a). In June the lowest ratios were

observed in plumes in the Irish Sea (Boxes VII and VIII in Fig. 2b) and downwind of London (Box IV in Fig. 2b) and there was a broader region of elevated O_3-NO_x in the south (Box V and regions to the west in Fig. 2b). The low ratio locations coincided with where the UK4 model and backward trajectories predicted plume transport from urban areas. The elevated region in the south during the June flights corresponded with European and southern UK outflow. Ozone-to-NO_x ratios were generally higher in June compared to April, reflecting the larger contribution from aged air masses and greater amount of sunlight available for photochemistry.

3.3 Aerosol mass concentrations and composition

We calculated total sub-micron aerosol mass as the sum of OA, nitrate, sulfate, ammonium and non-sea salt chloride measured by the AMS and rBC mass measured by the SP2 (Figs. 2c and d). Aerosol mass concentrations were higher in June compared to April, with maximum concentrations of approximately 25 $\mu g\,sm^{-3}$ measured in the European outflow sampled to the south of the UK, shown in Fig. 2d. Mass concentrations in the urban plumes sampled downwind of London and northern England were similar for both days, with concentrations on the order of 10–15 $\mu g\,sm^{-3}$. Clean background concentrations observed to the west of northern Wales were less than 5 $\mu g\,sm^{-3}$ on both days.

The aerosol composition varied across different regions, with urban/near-source plumes having higher rBC mass concentrations compared to background concentrations and European/regional pollution, as shown in Fig. 3a–b. The rBC mass concentration in the London and Liverpool/Manchester plumes was on the order of 0.5–1 $\mu g\,sm^{-3}$ compared to 0.1 $\mu g\,sm^{-3}$ (background) and 0.2 $\mu g\,sm^{-3}$ (European regional). Organic aerosol, nitrate and sulfate mass concentrations (in the form of ammonium nitrate and ammonium sulfate determined from the ion balance), shown in Fig. 3c–h, were highest in the regional European outflow sampled in June, but all three species also had higher mass concentrations in the urban plumes compared to background concentrations on both days. Nitrate was approximately 7 times higher in the London plume compared to background and both sulfate and OA were approximately twice as high.

The composition of the OA component also varied with location and between the two days, based on the PMF analysis. Figure 4 shows the OOA fraction of OA for both days. HOA mass concentrations were highest in urban plumes while OOA was higher in background and/or regional aerosol, though OOA was also observed in urban plumes. OOA was a slightly lower fraction of OA (approximately 40–50 %) for the April flight compared to the June flights, when it was between 50–60 % of OA in urban plumes and over 90 % in the regional and background aerosol.

Increases in OOA have been previously related to photochemical activity, which is higher in summer due to the longer days and increased actinic flux. Higher OOA in the summer is also consistent with the hypothesis that most of the OOA is derived from biogenic precursors that require interaction with anthropogenic pollution to enhance secondary organic aerosol concentrations (Spracklen et al., 2011). Most previous AMS measurements in and downwind of UK cities took place during winter and showed major contributions by traffic, solid fuel burning and cooking to OA (Allan et al., 2010; Liu et al., 2011). Allan et al. (2003) performed summertime AMS measurements in Manchester that were later re-analyzed using PMF by Jimenez et al. (2009), who determined that OOA represented approximately 60 % of OA, consistent with our observations in the northwestern plumes in June. During winter the OOA contribution to OA in Manchester dropped to approximately 40 %, similar to the April measurements. Measurements of regional pollution across Europe in the summer have shown that OOA makes up approximately 90 % of OA (Morgan et al., 2010a), consistent with our measurements in regional pollution.

We examined aerosol composition in specific regions shown by boxes in Fig. 2a by calculating the average mass fractions for each species. The box-averaged air mass properties are shown in Table 1 and Fig. 5 for both days. Sulfate and ammonium mass fractions were relatively constant in different locations and for both days, together representing approximately 40 % of the sub-micron aerosol. In April, nitrate was the major species, making up about 40 % of aerosol mass in the urban plumes and slightly less in the background aerosol. Organic aerosol was about 10–20 % of the mass, with roughly equal contributions by HOA and OOA and slightly higher OOA values in the background aerosol compared to the urban plumes in June. The differences in April were less clear, partly due to the lower OA mass concentrations. rBC was 3–4 % of the mass, with higher mass fractions in the urban plumes compared to background aerosol. The main difference in composition in June was the increase in OA at the expense of nitrate. Together HOA and OOA represented about 20–30 % of sub-micron mass in plumes and European outflow and almost 50 % of mass in the background aerosol. Refractory BC mass fractions in plumes were similar to those observed in April, but we observed lower rBC mass fractions in the European outflow (1 %) and background aerosol (2 %). Sulfate concentrations were elevated in the NW plume 1 (Box VII) compared to other regions sampled in June. We believe this plume originated from coal-fired power plants, but also had contributions from other sources.

3.4 Black carbon mixing state

We observed a clear decrease in f for rBC measured in urban plumes compared to rBC measured in other regions around the UK on both days, shown in Fig. 6. The regions with lower f coincided with areas of low O_3-to-NO_x ratios and where the UK4 visibility model and backward trajectory analysis (not shown) predicted transport from urban locations. Air

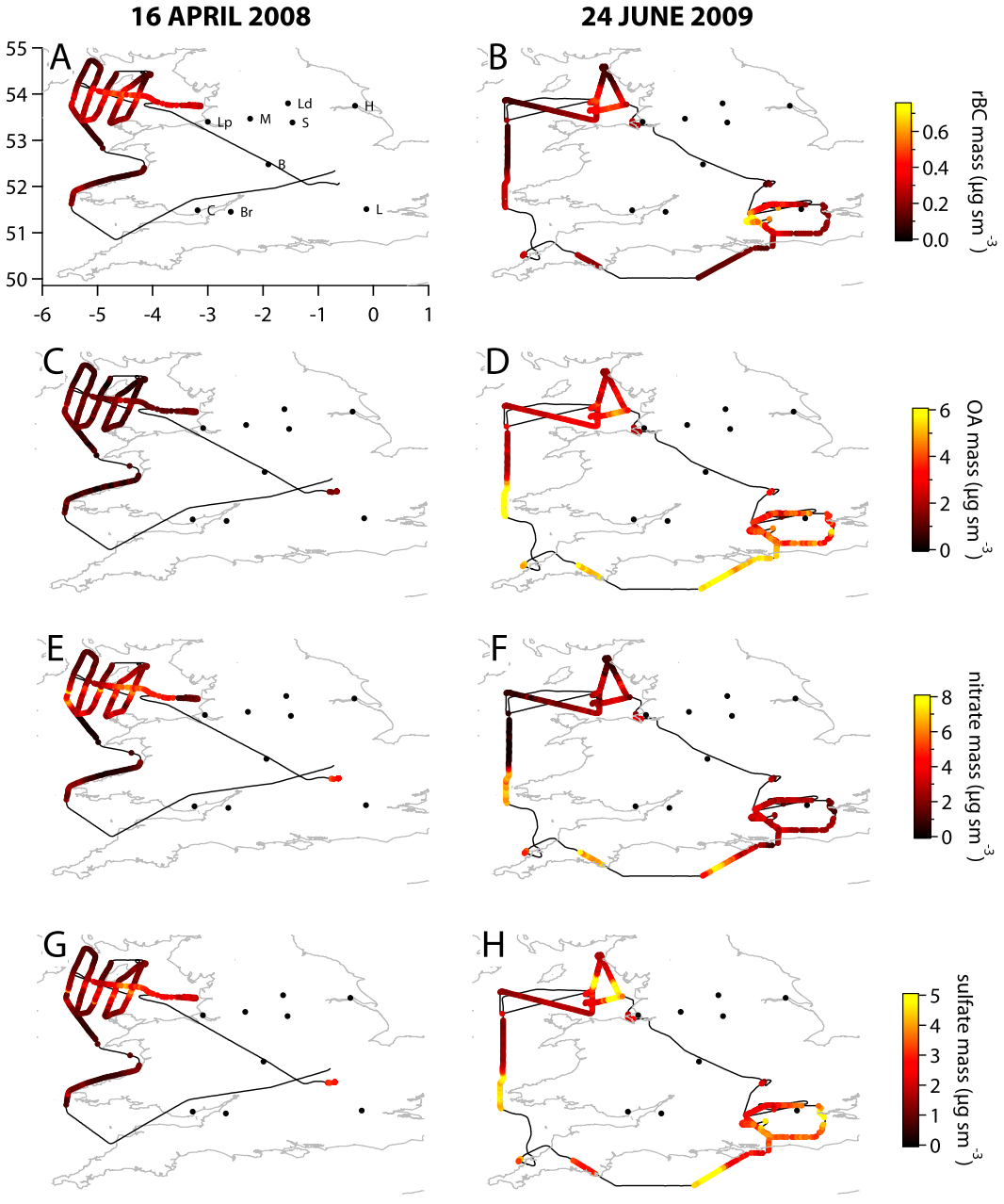

Fig. 3. Maps showing mass concentrations of **(a–b)** refractory black carbon (rBC), **(c–d)** organic aerosols (OA), **(e–f)** nitrate, and **(g–h)** sulfate measured during level runs inside the boundary layer for each day. Locations of major cities are also shown and labeled as: L, London; B, Birmingham; Br, Bristol; C, Cardiff; Lp, Liverpool; M, Manchester; Ld, Leeds; S, Sheffield; H, Kingston-upon-Hull.

masses sampled in the Irish Sea to the northwest of Liverpool in April had passed over the Liverpool/Manchester area less than 6 h prior to sampling. We conclude that the rBC particles sampled here were relatively fresh rBC emissions in urban plumes. We classified between 10–20 % of the rBC in urban plumes as "thickly coated" compared to 25–50 % in the background rBC and European outflow. Refractory BC sampled in the Bristol plume in April had slightly higher f which may be related to the slightly longer transport time between the sampling location and the expected source region.

Several recent studies have examined the rBC mixing state around and downwind of major cities. Schwarz et al. (2008a) performed a time-delay analysis to examine rBC properties over Texas and found a similar distinction between urban emissions (f = 3–15 %) and background/continental rBC (f = 40–50 %) as we observed over the UK. Moteki et al.

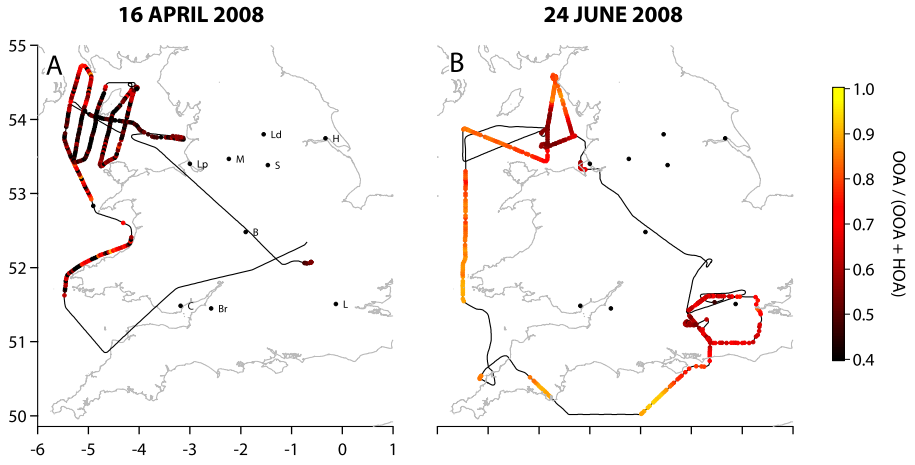

Fig. 4. Maps showing the oxidized organic aerosol (OOA) fraction of organic aerosol (OA) determined from positive matrix factorization of AMS organic mass spectra.

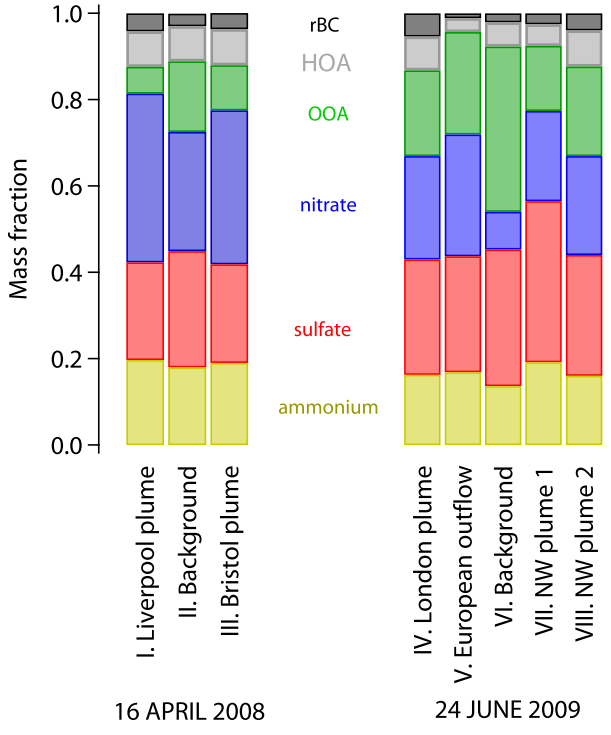

Fig. 5. Mass concentrations and mass fractions of rBC, HOA, OOA, nitrate, sulfate and ammonium averaged over different regions of the 16 April 2008 and 24 June 2009 flights shown in Figure 2a.

(2007) and Subramanian et al. (2010) measured f downwind of Tokyo and Mexico City, respectively and observed increases in f as the plumes aged. Moteki et al. (2007) found that f in the Tokyo plume increased at 2.3 % h^{-1} but Subramanian et al. (2010) observed a slower rate downwind of Mexico City (< 0.5 % h^{-1}). Our flights did not track transformations in a single plume, but rather sampled different plumes at varying distances downwind of the expected source regions. We estimated the air mass transport time by examining backward trajectories originating from various points along the flight track and compared these with f. The air mass transport time was only a rough estimate because of uncertainties on the source region, but we still found a correlation (Pearson's r^2 = 0.65) between air mass age and f. It increased by approximately 1 % h^{-1}, slower than the Tokyo observations but higher than those for Mexico City. There are a number of possible explanations for these differences. The photochemical environment over the UK is different from that downwind of Mexico City. Less light is available for photochemical reactions due to the higher latitude and lower elevation and VOC concentrations may be different, though we lack VOC observations to confirm this. The photochemical environment affects the formation of secondary organic aerosol (SOA) and associated condensation onto pre-existing rBC particles. The initial rBC mixing state of the rBC emissions may differ between Japan, the UK, and Mexico City due to different rBC sources, leading to different mixing rates downwind. Coagulation rates and potential cloud processing could also play a role, though we lacked sufficient information to make any detailed comparisons across sites.

3.5 Aerosol optical properties

We measured aerosol light absorption and scattering coefficients using the PSAP and integrating nephelometer. The PSAP uses a filter to sample particles, which can lead to a number of artifacts in the measurement, even after the application of standard correction procedures. We discussed these in more detail in McMeeking et al. (2010), but to summarize briefly we expect larger overestimates of the true absorption

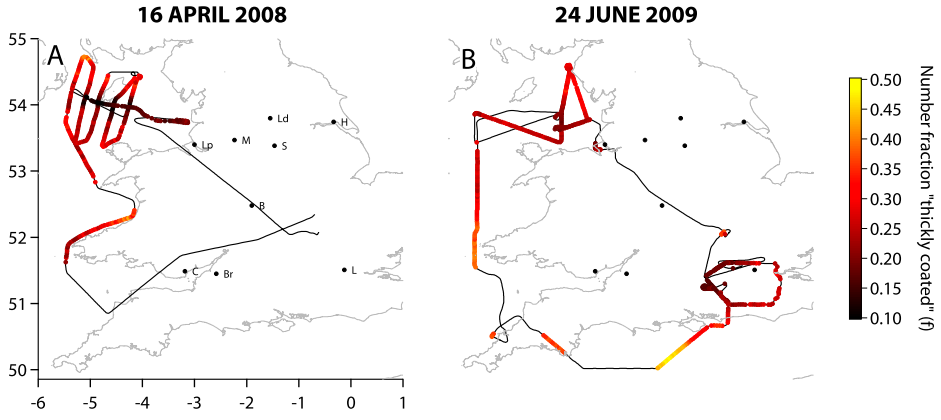

Fig. 6. Maps showing the number fraction of thickly coated rBC particles determined from a time delay analysis of single particle incandescence and scattering signals for 16 April 2008 and 24 June 2009.

coefficient in regions with large concentrations of organic aerosol (Subramanian et al., 2007; Lack et al., 2008; Cappa et al., 2008) that remain even after applying common correction procedures (e.g., Bond et al., 1999; Virkkula et al., 2005).

Light absorption coefficients, corrected to STP, were correlated with rBC mass concentrations on both days (Pearson's r^2 = 0.78 and 0.69 for April and June, respectively). The regressions of light absorption coefficient on rBC mass, which give the average rBC mass absorption efficiency (MAE), were 15.4 ± 0.9 (regression coefficient ±95 % confidence interval) and $11.4 \pm 0.7\,m^2\,g^{-1}$ for the April and June flights, respectively. Subramanian et al. (2010) measured MAEs of 10.6 ± 2.3 and $11.3 \pm 3.1\,m^2\,g^{-1}$ at λ = 660 nm in fresh outflow and 1-day old air masses over and downwind of Mexico City. Converting the Mexico City measurements to λ = 550 nm assuming a λ^{-1} wavelength dependence (Subramanian et al., 2010) gave MAE = 12.7 ± 2.8 and $13.6 \pm 3.7\,m^2\,g^{-1}$, within the range of our UK measurements.

As Subramanian et al. (2010) discussed, these MAE values are larger than expected for fresh combustion soot ($7.5 \pm 1.2\,m^2\,g^{-1}$), and in some cases larger than the 50 % enhancement expected for coated soot based on theoretical considerations (Bond and Bergstrom, 2006; Lack and Cappa, 2010) or laboratory measurements of simple coated absorbing core systems (Lack et al., 2009). Shiraiwa et al. (2010) showed absorption enhancements as large as 2 for coated graphite particles, but these experiments did not account for the role of fractal soot structures and their potential collapse when coated, which affects their absorption efficiency. Schwarz et al. (2008b) calculated absorption enhancements on the order of 30 % using SP2 measurements of rBC coating thickness and Mie theory, however these calculations also do not capture the effects of potential changes in rBC core shape with the additions of coating.

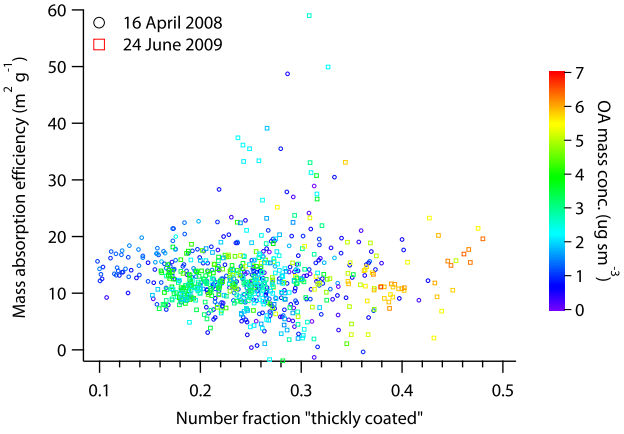

Fig. 7. Refractory black carbon (rBC) mass absorption efficiency calculated from SP2 measured rBC mass concentrations and corrected PSAP-measured light absorption coefficients at λ = 550 nm and standard temperature and pressure as a function of the number fraction of thickly coated particles measured by the SP2. Points are shaded by organic aerosol mass concentrations measured by the AMS. Each day is plotted using a different symbol. Only measurements inside the boundary layer are plotted.

To investigate potential causes of the large MAE values we examined relationships between MAE and f for both flight days, shown in Fig. 7. We did not observe any increase in MAE with respect to changes in f on either day. Biases in PSAP measurements have been observed to increase with increasing OA mass concentrations (Lack et al., 2008; Cappa et al., 2008), but we found no significant relationship between MAE and OA mass. We observed OA concentrations between 1–7 $\mu g\,sm^{-3}$. Lack et al. (2008) measured PSAP biases between approximately 1.3–1.5 in this range, so our ability to detect an erroneous change of this magnitude may be limited by the measurement variability.

The high MAE values may also result partially from an underestimate in rBC mass concentrations due to the limited size range of the SP2. Unlike Subramanian et al. (2010), we did not apply a correction factor for mass falling outside the SP2 detection range. Previously applied adjustments to account for rBC mass outside the detection range typically fall between 1.3–1.5, which would reduce our average MAE values to between 8.5–12 $m^2\,g^{-1}$, closer to theoretical and previously measured values. Physical increases in MAE coinciding with shifts in the rBC core mass distribution that result in a higher fraction of rBC particles being detected by the SP2 could give a relatively constant MAE (Subramanian et al., 2010). The SP2 would measure more of the total rBC mass for a larger diameter rBC population compared to a smaller diameter population with identical total mass concentration and absorption coefficient. The resulting calculated MAE would be lower, even if the true MAE were constant. Physically, Mie theory shows that the MAE can change with particle diameter due to interactions between the incident radiation and absorbing region of the particle (Bond and Bergstrom, 2006). For these effects to offset the expected amplification due to mixing, changes in mixing state resulting in more thickly coated rBC particles would have to coincide with increases in the rBC mass size distribution. To test this, we compared MAE to the mean geometric diameters calculated for rBC cores detected by the SP2 on 24 June. We observed a weak decrease in MAE for increasing rBC mean diameters ($-0.1 \pm 0.1\,m^2\,g^{-1}\,nm^{-1}$) with a low correlation (Pearson's r^2 = 0.02). Thus though we might expect a small change in MAE due to shifts in the rBC mass distribution, they were not large enough to offset the expected 30–50 % increase in absorption. Large amounts of small rBC particles below the detection limit of the SP2 could still play a role in explaining the lack of observed changes in MAE, but we are unable to comment further given the instrument limitations.

To summarize our discussion of the MAE values observed during the two days, we did not observe a significant change in MAE for differences in f or parameters related to f, such as the OOA fraction of OA or the ozone-to-NO_x ratio. There are several instrumental and physical reasons that could explain the lack of observed changes. From an instrumental perspective, biases in the PSAP may prevent physical changes in absorption from being detected with enough accuracy, as discussed by Subramanian et al. (2010). The SP2 mass measurement may underestimate the rBC mass for periods when the size distribution had greater contributions from relatively fresh, small rBC particles. Such an error results in erroneously high MAE, but we did not observe any clear evidence for changes in rBC mass distributions affecting calculated MAE. The f parameter may not capture important changes in the rBC mixing state that affect absorption. The lack of MAE changes could also be physical as opposed to artificial. Our aircraft observations may not have measured "fresh" non-coated BC that one might observe very close to the source. If this was the case our observations simply showed a lack of further enhancement of absorption beyond the initial mixing. The rBC cores may collapse as they become thickly coated, lessening the absorption enhancement of the coating (Bond and Bergstrom, 2006). The coating material may be partially absorbing, also reducing the absorption enhancement by directing fewer photons to the rBC core (Lack and Cappa, 2010). Despite this, the addition of non-rBC light absorbing material would lead to an increase in calculated MAE because its calculation assumes rBC is the only light absorbing material present in the aerosol. We expect the effect to be more important in biomass burning impacted regions where brown carbon plays an important role.

The single scattering albedo (SSA) is the ratio of light scattering to extinction and is an important parameter when determining the radiative forcing of aerosols. We calculated SSA from measured light scattering and absorption coefficients, both corrected to STP and for well-known instrument artifacts. The PSAP correction procedure provided by Bond et al. (1999) also adjusted the absorption coefficient measured λ = 567 nm to 550 nm, which was needed to compare with the scattering coefficient measured λ = 550 nm. The magnitude of the correction was <3 %; see discussion in Ogren (2010) for details. We were interested to see how changes in the rBC mixing state and relative abundance of rBC and non-absorbing species affected the SSA (Fig. 8a). SSA and rBC mass fractions were negatively correlated as expected because rBC was the major light-absorbing species during the flights. The addition of non-absorbing secondary aerosol mass, such as ammonium nitrate, ammonium sulfate and OOA led to higher aerosol scattering coefficients and higher SSA. SSA typically varied from 0.85 in urban plumes to 0.9–0.95 in the regional pollution and background aerosol. We estimated the relative contributions of OA, nitrate and sulfate to changes in SSA by assuming they were the only light scattering aerosol components and comparing their concentrations inside and outside of the urban plumes. Nitrate and OOA were the two largest contributors to increases in SSA, each responsible for approximately 30 % of the increased scattering aerosol mass.

We also show the SSA as a function of the rBC mixing state represented by the parameter f in Fig. 8b. For both days, we observed increases in SSA as f increased, meaning the increase in the scattering coefficient resulting from the addition of secondary aerosols more than compensated for any possible increases in the absorption coefficient arising from changes in the rBC mixing state. If the increase in MAE was due to OA-related PSAP measurement artifacts then we would expect to see an even larger increase in the real SSA for higher f values because these corresponded to periods with higher OA concentrations. This does not mean the changes in rBC optical properties with age should be ignored, however. If the rBC MAE increases with age due to changes in mixing state, the changing MAE must still be represented accurately in radiative forcing calculations, otherwise the predicted SSA will be too large.

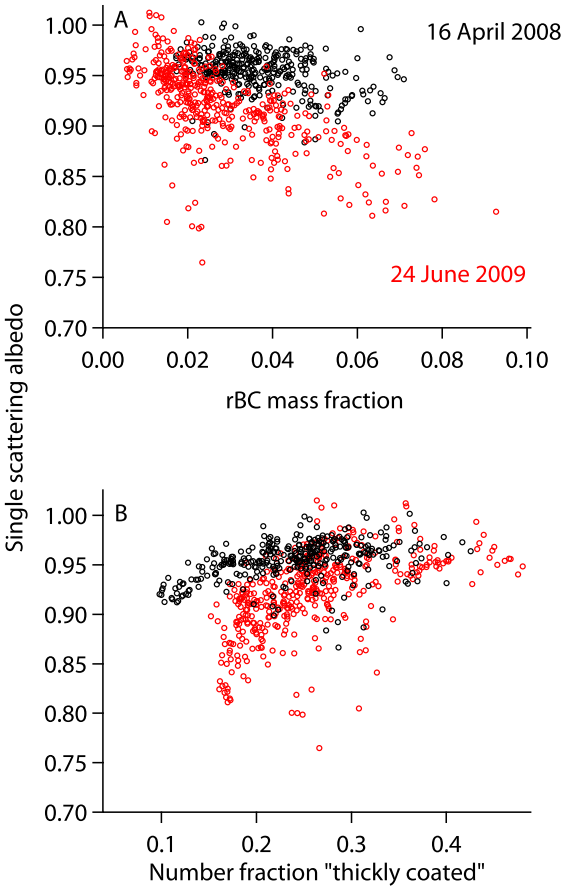

Fig. 8. Aerosol single scattering albedo calculated as the ratio of light scattering coefficients to total extinction coefficients plotted as a function of the rBC mass fraction of total sub-micron mass and the number fraction of thickly coated rBC particles detected by the SP2.

3.6 Aerosol vertical structure

Most of the sampling took place in the boundary layer, but we did perform several profile ascents and descents to examine the vertical structure in aerosol composition. Horizontal differences in aerosol composition can complicate the interpretation of the vertical structure because the profiles are performed over a significant horizontal distance during aircraft measurements. We performed profiles in the vicinity of Liverpool in April (Fig. 9a) and in the vicinity of London (Fig. 9b) and Liverpool (Fig. 9c) in June. Refractory black carbon concentrations remained relatively constant throughout the layer closest to the surface for all three profiles. The April profile was truncated at about 800 m altitude due to an altitude-dependent response problem with the instrument, but the June flights show rBC mass concentrations decreasing at approximately 700 m over London in the morning and at approximately 2000 m over Liverpool in the afternoon. A second more dilute layer of elevated rBC mass concentrations lay between the top of the surface layer and 1700 m over London.

The AMS-measured sub-micron aerosol mass composition and concentrations displayed more structure within the boundary layer. In April sulfate, nitrate and OA remained relatively constant before decreasing at approximately 1200 m. In June, OA, sulfate and nitrate increased between 1000–2000 m compared to their near surface values over London. There was a weaker increase over Liverpool, with sulfate concentrations decreasing and OA increasing slightly. Nitrate mass concentrations increased from less than 1 $\mu g\,sm^{-3}$ near the surface to 6 $\mu g\,sm^{-3}$ over London and approximately 3 $\mu g\,sm^{-3}$ over Liverpool. Morgan et al. (2009) and Morgan et al. (2010b) also observed increased nitrate concentrations near the top of the boundary layer and suggested they were related to the temperature- and relative humidity-dependent equilibrium of the ammonia-nitric acid-ammonium nitrate system. The increase observed over London was probably a combination of semi-volatile nature of nitrate and changes in air mass age/origin because non-volatile sulfate and rBC mass concentrations also change.

The rBC mixing state also displayed a strong altitude dependence, with higher f values observed above the boundary layer for the 24 June profiles. Figure 9b shows that rBC in the lowest 800 m near the surface had low f as expected for fresh emissions. The mixing state for rBC above this layer was similar to that observed in aged air masses, with f of approximately 0.3–0.5, similar to that observed in the free troposphere above. The rBC in this layer was likely aged rBC in the residual layer transported from sources upwind. The profile over Liverpool from later that day shows that the growth of the boundary layer has transported relatively fresh rBC with low f to as high as 1800 m. The rBC mixing state above this layer in the free troposphere has $f > 0.5$, suggesting it was more highly aged.

4 Conclusions

We have presented airborne observations of sub-micron aerosol composition and optical properties over the UK in April 2008 and June 2009, including rBC mixing state. We found higher concentrations of rBC in urban plumes that also had a relatively low fraction of thickly coated rBC particles. The plumes also had higher fractions of HOA and lower ozone-to-NO_x ratios. We did not observe any clear changes in rBC properties within individual plumes, but did observe significant differences between the plumes and surrounding regions. We estimated that rBC became "thickly coated" at a rate of 1 % h^{-1} downwind of UK and European source regions, approximately half the rate observed downwind of Tokyo, but higher than observed downwind of Mexico City. Refractory black carbon in background regions and in European continental outflow had a higher fraction of

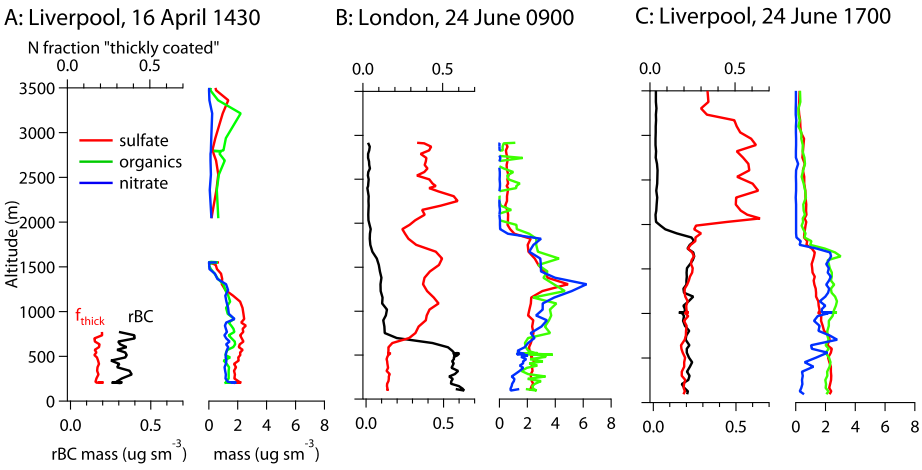

Fig. 9. Refractory black carbon (rBC) and sub-micron aerosol concentrations, composition and mixing state shown as a function of altitude in the vicinity of **(a)** Liverpool, England (approx. 14:30 UTC on 16 April 2008), **(b)** London, England (approx. 09:00 UTC on 24 June 2009) and **(c)** Liverpool, England (approx. 17:00 UTC on 24 June 2009). All profiles are shown on the same scales.

thickly coated particles. These regions also had higher fractions of OOA, higher ozone-to-NO_x ratios and higher sub-micron aerosol mass concentrations.

We found no evidence of an increase in the mass absorption efficiency of rBC in more aged and oxidized air masses, despite observing significant changes in the rBC mixing state and aerosol composition. This could be related to limitations in the PSAP-based absorption measurement, the size limitations of the SP2, or it could be a physical effect whereby the acquisition of coatings is offset by collapse of the rBC core. Regardless of the cause, two independent measurements (our study and Subramanian et al., 2010) have failed to observe any significant increase in the MAE of rBC downwind of urban sources and additional measurements are urgently needed to verify or refute these findings given their implications for radiative forcing calculations. Observations downwind of UK urban regions during different times of the year (e.g., winter) and different transport patterns (e.g., westerlies) could establish if our limited number of observations represent typical aging behavior or only represent spring/summer conditions under easterly flow. Even if rBC optical properties are shown to be relatively constant in this and other regions, changes in mixing state will still need to be represented due their influences on rBC hygroscopicity and lifetime, thus additional measurements similar to these are still needed.

Acknowledgements. The ADIENT project was supported by the UK Natural Environment Research Council (NERC; NE/E011101/1). The EM25 project was supported by the UK Meteorological Office. WTM was supported by a a NERC studentship (NER/S/A/2006/14040) and a CASE sponsorship from Aerodyne Research Inc. Airborne data were obtained using the BAe-146-301 large Atmospheric Research Aircraft (ARA) flown by Directflight Ltd. and managed by the Facility for Airborne Atmospheric Measurements (FAAM), which is a joint facility of NERC and the Met Office. We thank the ADIENT team members and Avalon Engineering for their contributions to the campaigns. Re-analysis data were provided by the ECMWF. The authors gratefully acknowledge the NOAA Air Resources Laboratory (ARL) for the provision of the HYSPLIT transport and dispersion model and READY website (http://www.arl.noaa.gov/ready.php) used in this publication.

Edited by: R. Krejci

References

Allan, J. D., Alfarra, M. R., Bower, K. N., Williams, P. I., Gallagher, M. W., Jimenez, J. L., McDonald, A. G., Nemitz, E., Canagaratna, M. R., Jayne, J. T., Coe, H., and Worsnop, D. R.: Quantitative sampling using an Aerodyne Aerosol Mass Spectrometer 2. Measurements of fine particulate chemical composition in two U.K. cities, J. Geophys. Res., 108, 4091, doi:10.1029/2002JD002359, 2003.

Allan, J. D., Williams, P. I., Morgan, W. T., Martin, C. L., Flynn, M. J., Lee, J., Nemitz, E., Phillips, G. J., Gallagher, M. W., and Coe, H.: Contributions from transport, solid fuel burning and cooking to primary organic aerosols in two UK cities, Atmos. Chem. Phys., 10, 647–668, doi:10.5194/acp-10-647-2010, 2010.

Anderson, T. L. and Ogren, J. A.: Determining aerosol radiative properties using the TSI 3563 integrating nephelometer, Aerosol Sci. Tech., 29, 57–69, 1998.

Baumgardner, D., Kok, G., Kramer, M., and Weidle, F.: Meridional gradients of light absorbing carbon over northern Europe, Environ. Res. Lett., 3, 025010, doi:10.1088/1748-9326/3/2/025010, 2008.

Bond, C. M., Anderson, T. L., and Campbell, D.: Calibration and intercomparison of filter-based measurements of visible light absorption by aerosols, Aerosol Sci. Technol., 30, 582–600, 1999.

Bond, T. and Bergstrom, R.: Light absorption by carbonaceous particles: An investigative review, Aerosol Sci. Technol., 40, 27–67, doi:10.1080/02786820500421521, 2006.

Cappa, C. D., Lack, D. A., Burkholder, J. B., and Ravishankara, A. R.: Bias in filter-based aerosol light absorption measurements due to organic aerosol loading: Evidence from laboratory measurements, Aerosol Sci. Technol., 42, 1022–1032, doi:10.1080/02786820802389285, 2008.

Clark, P. A., Harcourt, S. A., Macpherson, B., Mathison, C. T., Cusack, S., and Naylor, M.: Prediction of visibility and aerosol within the operational Met Office Unified Model. I: Model formulation and variational assimilation, Q. J. Roy. Meteor. Soc., 134, 1801–1816, doi:10.1002/qj.318, 2008.

Dall'Osto, M., Ceburnis, D., Martucci, G., Bialek, J., Dupuy, R., Jennings, S. G., Berresheim, H., Wenger, J., Healy, R., Facchini, M. C., Rinaldi, M., Giulianelli, L., Finessi, E., Worsnop, D., Ehn, M., Mikkilä, J., Kulmala, M., and O'Dowd, C. D.: Aerosol properties associated with air masses arriving into the North East Atlantic during the 2008 Mace Head EUCAARI intensive observing period: an overview, Atmos. Chem. Phys., 10, 8413–8435, doi:10.5194/acp-10-8413-2010, 2010.

Draxler, R. R. and Rolph, G. D.: HYSPLIT (HYbrid Single-Particle Lagrangian Integrated Trajectory) Model access via NOAA ARL READY website (http://ready.arl.noaa.gov/HYSPLIT.php), 2011.

Drewnick, F., Hings, S. S., DeCarlo, P., Jayne, J. T., Gonin, M., Fuhrer, K., Weimer, S., Jimenez, J. L., Demerjian, K. L., Borrmann, S., and Worsnop, D. R.: A new time-of-flight aerosol mass spectrometer (TOF-AMS) – Instrument description and first field deployment, Aerosol Sci. Technol., 39, 637–658, 2005.

Fuller, K. A., Malm, W. C., and Kreidenweis, S. M.: Effects of mixing on extinction by carbonaceous particles, J. Geophys. Res.-Atmos., 104, 15941–15954, 1999.

Haywood, J. M. and Osborne, S. R.: Estimates of the direct and indirect radiative forcing due to tropospheric aerosols: A review, Rev. Geophys., 38, 513–543, 2000.

Haywood, J. M., Bush, M., Abel, S., Claxton, B., Coe, H., Crosier, J., Harrison, M., Macpherson, B., Naylor, M., and Osborne, S.: Prediction of visibility and aerosol within the operational Met Office Unified Model II: Validation of model performance using observational data, Q. J. Roy. Meteor. Soc., 134, 1817–1832, 2008.

Jacobson, M. Z.: Short-term effects of controlling fossil-fuel soot, biofuel soot and gases, and methane on climate, Arctic ice, and air pollution health, J. Geophys. Res., 115, D14209, doi:10.1029/2009JD013795, 2010.

Jimenez, J. L., Canagaratna, M. R., Donahue, N. M., Prevot, A. S. H., Zhang, Q., Kroll, J. H., DeCarlo, P. F., Allan, J. D., Coe, H., Ng, N. L., Aiken, A. C., Docherty, K. S., Ulbrich, I. M., Grieshop, A. P., Robinson, A. L., Duplissy, J., Smith, J. D., Wilson, K. R., Lanz, V. A., Hueglin, C., Sun, Y. L., Tian, J., Laaksonen, A., Raatikainen, T., Rautiainen, J., Vaattovaara, P., Ehn, M., Kulmala, M., Tomlinson, J. M., Collins, D. R., Cubison, M. J., Dunlea, E. J., Huffman, J. A., Onasch, T. B., Alfarra, M. R., Williams, P. I., Bower, K., Kondo, Y., Schneider, J., Drewnick, F., Borrmann, S., Weimer, S., Demerjian, K., Salcedo, D., Cottrell, L., Griffin, R., Takami, A., Miyoshi, T., Hatakeyama, S., Shimono, A., Sun, J. Y., Zhang, Y. M., Dzepina, K., Kimmel, J. R., Sueper, D., Jayne, J. T., Herndon, S. C., Trimborn, A. M., Williams, L. R., Wood, E. C., Middlebrook, A. M., Kolb, C. E., Baltensperger, U., and Worsnop, D. R.: Evolution of organic aerosols in the atmosphere, Science, 326, 1525–1529, doi:10.1126/science.1180353, 2009.

Koch, D., Schulz, M., Kinne, S., McNaughton, C., Spackman, J. R., Balkanski, Y., Bauer, S., Berntsen, T., Bond, T. C., Boucher, O., Chin, M., Clarke, A., De Luca, N., Dentener, F., Diehl, T., Dubovik, O., Easter, R., Fahey, D. W., Feichter, J., Fillmore, D., Freitag, S., Ghan, S., Ginoux, P., Gong, S., Horowitz, L., Iversen, T., Kirkevåg, A., Klimont, Z., Kondo, Y., Krol, M., Liu, X., Miller, R., Montanaro, V., Moteki, N., Myhre, G., Penner, J. E., Perlwitz, J., Pitari, G., Reddy, S., Sahu, L., Sakamoto, H., Schuster, G., Schwarz, J. P., Seland, Ø., Stier, P., Takegawa, N., Takemura, T., Textor, C., van Aardenne, J. A., and Zhao, Y.: Evaluation of black carbon estimations in global aerosol models, Atmos. Chem. Phys., 9, 9001–9026, doi:10.5194/acp-9-9001-2009, 2009.

Koschmieder, H: Theorie der horizontalen Schweite, Beitraege zur Physik der Atmosphaere, 12, 33–53, 1924.

Lack, D., Cappa, C., Covert, D., Baynard, T., Massoli, P., Sierau, B., Bates, T., Quinn, P., Lovejoy, E., and Ravishankara, A. R.: Bias in Filter-Based Aerosol Light Absorption Measurements Due to Organic Aerosol Loading: Evidence from Ambient Measurements, Aerosol Sci. Technol., 42, 1033–1041, doi:10.1080/02786820802389277, 2008.

Lack, D., Cappa, C., Cross, E., Massoli, P., Ahern, A., Davidovits, P., and Onasch, T.: Absorption Enhancement of Coated Absorbing Aerosols: Validation of the Photo-Acoustic Technique for Measuring the Enhancement, Aerosol Sci. Technol., 43, 1006–1012, doi:10.1080/02786820903117932, 2009.

Lack, D. A. and Cappa, C. D.: Impact of brown and clear carbon on light absorption enhancement, single scatter albedo and absorption wavelength dependence of black carbon, Atmos. Chem. Phys., 10, 4207–4220, doi:10.5194/acp-10-4207-2010, 2010.

Liu, D., Flynn, M., Gysel, M., Targino, A., Crawford, I., Bower, K., Choularton, T., Jurányi, Z., Steinbacher, M., Hüglin, C., Curtius, J., Kampus, M., Petzold, A., Weingartner, E., Baltensperger, U., and Coe, H.: Single particle characterization of black carbon aerosols at a tropospheric alpine site in Switzerland, Atmos. Chem. Phys., 10, 7389–7407, doi:10.5194/acp-10-7389-2010, 2010.

Liu, D., Allan, J., Corris, B., Flynn, M., Andrews, E., Ogren, J., Beswick, K., Bower, K., Burgess, R., Choularton, T., Dorsey, J., Morgan, W., Williams, P. I., and Coe, H.: Carbonaceous aerosols contributed by traffic and solid fuel burning at a polluted rural site in Northwestern England, Atmos. Chem. Phys., 11, 1603–1619, doi:10.5194/acp-11-1603-2011, 2011.

Matthew, B., Middlebrook, A. M., and Onasch, T. B.: Collection Efficiencies in an Aerodyne Aerosol Mass Spectrometer as a Function of Particle Phase for Laboratory Generated Aerosols, Aerosol Sci. Technol., 42, 884–898, 2008.

McMeeking, G. R., Hamburger, T., Liu, D., Flynn, M., Morgan, W. T., Northway, M., Highwood, E. J., Krejci, R., Allan, J. D., Minikin, A., and Coe, H.: Black carbon measurements in the boundary layer over western and northern Europe, Atmos. Chem. Phys., 10, 9393–9414, doi:10.5194/acp-10-9393-2010, 2010.

McMeeking, G. R., Good, N., Petters, M. D., McFiggans, G., and Coe, H.: Influences on the fraction of hydrophobic and hydrophilic black carbon in the atmosphere, Atmos. Chem. Phys.,

11, 5099–5112, doi:10.5194/acp-11-5099-2011, 2011a.

McMeeking, G. R., Bart. M., Chazette, P., Haywood, J. M., Highwood, E. J., McQuaid, J. B., Morgan, W. T., Raut, J.-C., Ryder, C. L., Savage, N., Trembath, J., Turnbull, K., and Coe, H.: Airborne measurements of trace gases and aerosols from around the London metropolitan region, in prep., 2011b.

Moffet, R. C. and Prather, K. A.: In-situ measurements of the mixing state and optical properties of soot with implications for radiative forcing estimates., Proceedings of the National Academy of Sciences of the United States of America, 106(29), 11872-11877, doi:10.1073/pnas.0900040106, 2009.

Morgan, W. T., Allan, J. D., Bower, K. N., Capes, G., Crosier, J., Williams, P. I., and Coe, H.: Vertical distribution of sub-micron aerosol chemical composition from North-Western Europe and the North-East Atlantic, Atmos. Chem. Phys., 9, 5389–5401, doi:10.5194/acp-9-5389-2009, 2009.

Morgan, W. T., Allan, J. D., Bower, K. N., Highwood, E. J., Liu, D., McMeeking, G. R., Northway, M. J., Williams, P. I., Krejci, R., and Coe, H.: Airborne measurements of the spatial distribution of aerosol chemical composition across Europe and evolution of the organic fraction, Atmos. Chem. Phys., 10, 4065–4083, doi:10.5194/acp-10-4065-2010, 2010a.

Morgan, W. T., Allan, J. D., Bower, K. N., Esselborn, M., Harris, B., Henzing, J. S., Highwood, E. J., Kiendler-Scharr, A., McMeeking, G. R., Mensah, A. A., Northway, M. J., Osborne, S., Williams, P. I., Krejci, R., and Coe, H.: Enhancement of the aerosol direct radiative effect by semi-volatile aerosol components: airborne measurements in North-Western Europe, Atmos. Chem. Phys., 10, 8151–8171, doi:10.5194/acp-10-8151-2010, 2010b.

Moteki, N. and Kondo, Y.: Effects of mixing state on black carbon measurement by laser-induced incandescence, Aerosol Sci. Technol., 41, 398–417, 2007.

Moteki, N., Kondo, Y., Miyazaki, Y., Takegawa, N., Komazaki, Y., Kurata, G., Shirai, T., Blake, D. R., Miyakawa, T., and Koike, M.: Evolution of mixing state of black carbon particles: Aircraft measurements over the western Pacific in March 2004, Geophys. Res. Lett., 34, L11803, doi:10.1029/2006GL028943, 2007.

Novelli, P. C., Masarie, K. A., and Lang, P. M.: Distributions and recent changes of carbon monoxide in the lower troposphere, J. Geophys. Res., 103, 19015–19033, doi:10.1029/98JD01366, 1998.

Ogren, J.: Comment on "Calibration and Intercomparison of Filter-Based Measurements of Visible Light Absorption by Aerosols", Aerosol Sci. Tech., 44, 589–591, doi:10.1080/02786826.2010.482111, 2010.

Paatero, P.: Least squares formation of robust non-negative factor analysis, Chemometrics and Intelligent Laboratory Systems, 37, 23–35, 1997.

Paatero, P. and Tapper, U.: Positive matrix factorization – A nonnegative factor model with optimal utilization of error-estimates of data values, Environmetrics, 5, 111–126, doi:10.1002/env.3170050203, 1994.

Pratt, K. A. and Prather, K. A.: Aircraft measurements of vertical profiles of aerosol mixing states, J. Geophys. Res., 115, D11305, 1–10, doi:10.1029/2009JD013150, 2010.

Riemer, N., West, M., Zaveri, R., and Easter, R.: Estimating black carbon aging time-scales with a particle-resolved aerosol model, J. Aerosol Sci., 41, 143–158, doi:10.1016/j.jaerosci.2009.08.009, 2010.

Rolph, G. D.: Real-time Environmental Applications and Display sYstem (READY) website (http://ready.arl.noaa.gov), 2011.

Schwarz, J. P., Gao, R. S., Fahey, D. W., Thomson, D. S., Watts, L. A., Wilson, J. C., Reeves, J. M., Darbeheshti, M., Baumgardner, D. G., Kok, G. L., Chung, S. H., Schulz, M., Hendricks, J., Lauer, A., Kaercher, B., Slowik, J. G., Rosenlof, K. H., Thompson, T. L., Langford, A. O., Loewenstein, M., and Aikin, K. C.: Single-particle measurements of midlatitude black carbon and light-scattering aerosols from the boundary layer to the lower stratosphere, J. Geophys. Res., 111, D16207, doi:10.1029/2006JD007076, 2006.

Schwarz, J. P., Gao, R. S., Spackman, J. R., Watts, L. A., Thomson, D. S., Fahey, D. W., Ryerson, T. B., Peischl, J., Holloway, J. S., Trainer, M., Frost, G. J., Baynard, T., Lack, D. A., de Gouw, J. A., Warneke, C., and Del Negro, L. A.: Measurement of the mixing state, mass, and optical size of individual black carbon particles in urban and biomass burning emissions, Geophys. Res. Lett., 35, L13810, doi:10.1029/2008GL033968, 2008a.

Schwarz, J. P., Spackman, J. R., Fahey, D. W., Gao, R. S., Lohmann, U., Stier, P., Watts, L. A., Thomson, D. S., Lack, D. A., Pfister, L., Mahoney, M. J., Baumgardner, D., Wilson, J. C., and Reeves, J. M.: Coatings and their enhancement of black carbon light absorption in the tropical atmosphere, J. Geophys. Res., 113, D03203, doi:10.1029/2007JD009042, 2008b.

Shiraiwa, M., Kondo, Y., Moteki, N., Takegawa, N., Miyazaki, Y., and Blake, D. R.: Evolution of mixing state of black carbon in polluted air from Tokyo, Geophys. Res. Lett., 34, L16803, doi:10.1029/2007GL029819, 2007.

Shiraiwa, M., Kondo, Y., Iwamoto, T., and Kita, K.: Amplification of Light Absorption of Black Carbon by Organic Coating, Aerosol Sci. Tech., 44, 46–54, doi:10.1080/02786820903357686, 2010.

Spracklen, D. V., Jimenez, J. L., Carslaw, K. S., Worsnop, D. R., Evans, M. J., Mann, G. W., Zhang, Q., Canagaratna, M. R., Allan, J., Coe, H., McFiggans, G., Rap, A., and Forster, P.: Aerosol mass spectrometer constraint on the global secondary organic aerosol budget, Atmos. Chem. Phys. Discuss., 11, 5699–5755, doi:10.5194/acpd-11-5699-2011, 2011.

Stephens, M., Turner, N., and Sandberg, J.: Particle identification by laser-induced incandescence in a solid-state laser cavity, Appl. Optics, 42, 3726–3736, 2003.

Subramanian, R., Roden, C. A., Boparai, P., and Bond, T. C.: Yellow Beads and Missing Particles: Trouble Ahead for Filter-Based Absorption Measurements, Aerosol Sci. Tech., 41, 630–637, doi:10.1080/02786820701344589, 2007.

Subramanian, R., Kok, G. L., Baumgardner, D., Clarke, A., Shinozuka, Y., Campos, T. L., Heizer, C. G., Stephens, B. B., de Foy, B., Voss, P. B., and Zaveri, R. A.: Black carbon over Mexico: the effect of atmospheric transport on mixing state, mass absorption cross-section, and BC/CO ratios, Atmos. Chem. Phys., 10, 219–237, doi:10.5194/acp-10-219-2010, 2010.

Ulbrich, I. M., Canagaratna, M. R., Zhang, Q., Worsnop, D. R., and Jimenez, J. L.: Interpretation of organic components from Positive Matrix Factorization of aerosol mass spectrometric data, Atmos. Chem. Phys., 9, 2891–2918, doi:10.5194/acp-9-2891-2009, 2009.

Virkkula, A., Ahlquist, N. C., Covert, D. S., Arnott, W. P., Sheridan, P. J., Quinn, P. K., and Coffman, D. J.: Modification, calibration

and a field test of an instrument for measuring light absorption by particles, Aerosol Sci. Tech., 39, 68–83, 2005.

Visschedijk, A. J. H., Zandveld, P., and Denier van der Gon, H. A.C.: A high resolution gridded European emission database for the EU integrated project GEMS, TNO-report 2007-A-R0233, 2007.

Weingartner, E., Burtscher, H., and Baltenspergert, U.: Hygroscopic properties of carbon and diesel soot particles, Atmos. Environ., 31, 2311–2327, 1997.

Wyslouzil, B. E., Carleton, K. L., Sonnenfroh, D. M., Rawlins, W. T., and Arnold, S.: Observation of hydration of single, modified carbon aerosols, Geophys. Res. Lett., 21, 2107–2110, 1994.

Zaveri, R. A., Barnard, J. C., Easter, R. C., Riemer, N., and West, M.: Particle-resolved simulation of aerosol size, composition, mixing state, and the associated optical and cloud condensation nuclei activation properties in an evolving urban plume, J. Geophys. Res., 115, D17210, 1–19, doi:10.1029/2009JD013616, 2010.

Zhang, Q., Jimenez, J. L., Canagaratna, M. R., Allan, J. D., Coe, H., Ulbrich, I., Alfarra, M. R., Takami, A., Middlebrook, A. M., Sun, Y. L., Dzepina, K., Dunlea, E. J., Docherty, K. S., Decarlo, P. F., Salcedo, D., Onasch, T., Jayne, J. T., Miyoshi, T., Shimono, A., Hatakeyama, S., Takegawa, N., Kondo, Y., Schneider, J., Drewnick, F., Borrmann, S., Weimer, S., Demerjian, K. L., Williams, P., Bower, K. N., Bahreini, R., Cottrell, L., Griffin, R. J., Rautiainen, J., Sun, J. Y., Zhang, Y. M., and Worsnop, D. R.: Ubiquity and dominance of oxygenated species in organic aerosols in anthropogenically-influenced Northern Hemisphere midlatitudes, Geophys. Res. Lett., 34, L13801, doi:10.1029/2007GL029979, 2007.

Zhang, R., Khalizov, A. F., Pagels, J., Zhang, D., Xue, H., and McMurry, P. H.: Variability in morphology, hygroscopicity, and optical properties of soot aerosols during atmospheric processing, P. Natl. A. Sci., 105, 10291–10296, doi:10.1073/pnas.0804860105, 2008.